0014-4754/96/080818-09$1.50 + 0.20

Characterization and relative abundance of maxi-chloride channels in Epstein-Barr virus (EBV) producer: B95-8 cells

T. H. Yeh[a,b,*], M. C. Tsai[b], S. Y. Lee[a] and M. M. Hsu[a]

[a] *Department of Otolaryngology, College of Medicine, National Taiwan University, Taipei (Taiwan)*
[b] *Department of Pharmacology, College of Medicine, National Taiwan University, Taipei (Taiwan)*
Received 25 July 1995; received after revision 5 October 1995; accepted 11 December 1995

Abstract. Several Epstein-Barr virus (EBV)-transformed cell lines were used to investigate the pathogenesis of lymphoproliferative diseases and nasopharyngeal carcinoma. The studies focus on the events occurring inside the membrane. On only one occasion, the cell membrane of EBV-transformed B lymphocytes from a cystic fibrosis patient was found to express defective Cl channels (CFTR; Cystic Fibrosis Transmembrane conductance Regulator), as in the airway epithelial cell. No other type of channel in EBV-transformed cells has so far been investigated. In this study, the cell membrane of the B95-8 cell was examined by the patch-clamp technique and compared to the non-EBV-infected BJAB cell. The high conductance (~300 pS) maxi-chloride (Cl) channel activity was the most frequently observed event in inside-out configurations. Under similar experimental conditions, we have found a significantly higher probability of detecting maxi-Cl channel activity on the cell membrane of B95-8 cells (69%) than on BJAB cells (27%), or as previously reported on resting murine B lymphocytes (38%) or intact human T lymphocytes (37%). The relative abundance of the maxi-Cl channel on B95-8 cells may be linked to EBV infection and/or secretory ability.
Key words. Epstein-Barr virus; anion channel; patch clamp.

Clinically, EBV is closely related to two notorious malignant diseases, nasopharyngeal carcinoma and Burkitt's lymphoma, which are common in southeast Asia and Africa respectively[1,2]. EBV is also well known for its ability to transform B lymphocytes in vitro. The B95-8 cell line was developed from polyclonal B lymphocytes of marmosets[3]. It can produce the Hawley strain of EBV particles[4]. EBV-transformed B cell lines are commonly used for studying the mechanism of EBV tumorigenesis.

Several lines of evidence indicate that EBV modulates the membrane of infected cells: 1) Marmoset transformants, including cell lines derived from malignant lymphoma, express neither the receptors for complement nor the receptors for the Fc fragment of immunoglobulin G[4]. 2) EBV obtained from B95-8 cells can upregulate some membrane proteins in cultured B lymphocytes. The structure of one of the proteins mimics a G-protein-related membrane receptor[5]. 3) One of the EBV gene products – latent membrane protein (LMP) – can transform rat fibroblasts in vitro[6]. The structure of LMP is similar to a voltage-gated potassium channel[7]. On the other hand, potassium channel blockers such as tetraethylammonium-Cl (TEA) or 4-aminopyridine (4-AP) can prevent mitogen-stimulated B lymphocytes proceeding from G_0 phase into S phase. Thus, the membrane channels may be involved in the process of lymphocyte activation[8].

* Corresponding author.

B lymphocytes of cystic fibrosis patients transformed by EBV expressed defective Cl channels, as in airway epithelial cells[9]. Other types of channels expressed after EBV infection have not been investigated. Furthermore, the M_2 protein of influenza virus, which facilitates the propagation of virus infection, has proved to be a non-selective cation channel[10,11]. These data indicate an intimate link between viral infection and cell membrane biology. Thus, investigating the channels located on the EBV-transformed cells may provide a new route to understanding the tumorigenesis of EBV. The purpose of this study was to characterize the membrane channel on B95-8 cells and compare it with non-EBV infected BJAB cells.

Materials and methods

Cell culture. B95-8 and BJAB cells were maintained in RPMI-1640 culture medium supplemented with penicillin/streptomycin (100 U/ml, 100 mg/ml) and 10% fetal calf serum. Cells were plated at a maximal density of 2×10^5 cells/petri dish (60 mm in diameter, Corning, NY, USA) and kept at 3 7 °C in a humidified atmosphere under 5% CO_2. The medium was changed every other day. Cells were used on the second to fourth day after transfer.

Electron microscopic study. The quality of the B95-8 cells was checked by electron microscopy. Cultured cells were collected after centrifugation. They were fixed for 2 h in 2.5% phosphate-buffered glutaraldehyde (pH = 7.4), then rinsed in buffer and postfixed in 1%

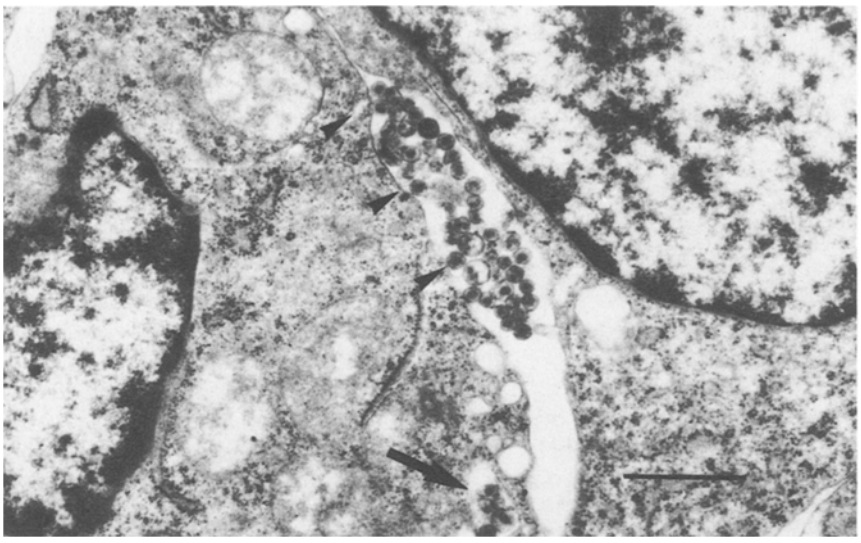

Figure 1. Electron microscopic findings in B95-8 cells. Large amounts of EBV particles are detected in the extracellular space (arrowheads). Intracellular vesicles containing some viral particles which seem readily to be excreted to the extracellular space (arrow) can be clearly seen. Bar represents 1 μm (original magnification ×7000).

phosphate-buffered osmium tetraoxide (pH = 7.4). After dehydration in graded concentrations of ethanol, cultured cells were embeded in Epon-araldite. Ultrathin sections were made, stained with uranyl citrate and examined with a Philips-400 electron microscope.

Patch-clamp experiments. Patch-clamp experiments were performed as described by Hamill et al.[12]. The petri dish containing cultured cells was perfused with a mammalian Ringer's solution containing (in mM): 140 NaCl, 4.8 KCl, 1 $CaCl_2$, 1.2 $MgCl_2$, 10 glucose and 10 hydroxyethyl-piperazine ethanesulphonic acid (HEPES), pH 7.4. This solution was also used as the pipette-filling solution. Patch pipettes were fabricated from borosilicate glass capillaries (Clark Electromedical Instruments, England) using a two-stage vertical pipette puller (Narishige, Japan) and coated with Sylgard 184 (Dow Corning, USA). Pipette resistances ranged from 4 to 8 MΩ. The cell-attached configuration was first obtained. Inside-out configuration was achieved following patch excision. The pipette tip was moved to the glass tube openings of a home-made perfusion system (perfusion rate: 4 ml/min) which permitted changing the cytoplasmic solution rapidly. The first cytoplasmic solution was 140 mM NaCl saline, and then 140 mM KCl saline (pH = 7.2). To study the anion versus cation selectivity, 400 mM NaCl saline, 42 mM NaCl (adding 200 mM sucrose to correct the osmolality) were used to measure the shift of reveral potential. To examine the relative selectivity of the channel for different anions, Cl^- in 140 mM NaCl saline was substituted by F^-, Br^-, I^- or gluconate. Inside-out patches also showed channel activity at different calcium concentrations from 10^{-9} to 10^{-3} M. Calcium concentrations of 10^{-6} M or less were adjusted with 100 mM ethylene glycol tetraacetic acid (EGTA) and 100 mM Ca-EGTA solutions. The reference agar bridge contained 1.5 M KCl. The junction potential varied with changes of the tested solution. These junction potentials were measured directly by a 3 M KCl electrode that had been zeroed with 140 mM NaCl saline in the bath. I–V relationships and reversal potentials were corrected for these offsets. The currents were recorded mainly in excised inside-out configuration using an Axopatch 1B (Axon Instrument) patch-clamp amplifier. Currents were low-pass-filtered at 10 kHz, played through a pulse-code modulator and stored using a video cassette recorder (Sony, SLV-393). During playback for inspection or analysis, currents were filtered with a 4-pole Bessel filter, and all records shown were at 1 kHz. The data were analyzed by pClamp software (version 5.5, Axon Instrument). Ionic current polarity was reported according to physiological convention, that is, positive charges leaving the cell (cation efflux, anion influx) corresponding to upward deflections in the illustrated single-channel recordings, and vice versa. Membrane potentials were reported as intracellular with respect to ground on the extracellular side. All appropriate numerical data were given as mean ±SE. Statistical figures were drawn using SigmaPlot 4.0 software. All experiments were carried out at room temperature (22–24 °C).

Chemicals. All solutions were prepared from commercial grade chemicals. The normal 140 mM NaCl saline was filtered through a 0.22 μm syringe filter immediately before use. The 4-acetamido-4′-isothiocyano-2,2′-disulphonic acid stilbene (SITS), 4,4′-diisothiocyano-2,2′-disulphonic acid stilbene (DIDS), $NiCl_2$ and $ZnCl_2$

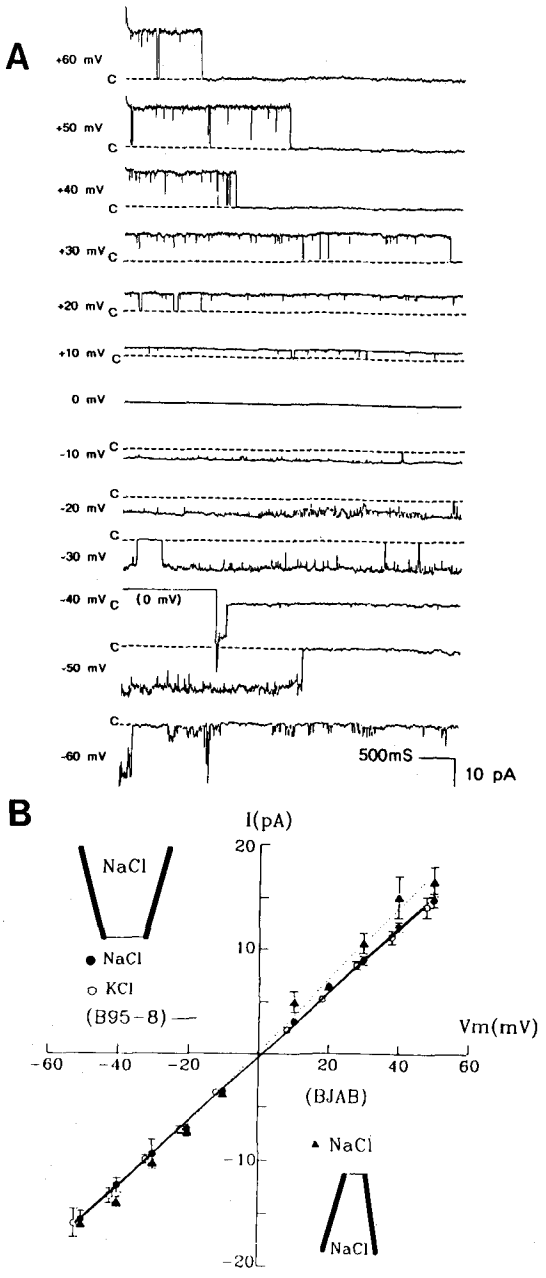

Figure 2. Activity of maxi-Cl channel in excised inside-out patches. (*A*) Single-channel recordings of an inside-out patch with one maxi-Cl channel obtained in symmetrical 140 mM NaCl solutions at different membrane potentials from a B95-8 cell. c and the dashes indicate the closed state of the channel. Note the rapid inactivation of the channel when the membrane potential steps from 0 mV to −40 mV. Some subconductance states were found in the −20 mV tracing. (*B*) I–V relationships for the maxi-Cl channel from B95-8 cells (NaCl in the cytoplasmic side, solid line, filled circles, n = 16; and KCl, solid line, open circles, n = 10) and BJAB cells (dashed line, filled triangles, n = 3). The data were fitted by a linear regression weighted by the SE of each point and exhibited similar unitary conductances, 316.7 ± 11.6 pS, 297.6 ± 15.1 pS and 343.6 ± 18.3 pS, respectively. The reversal potentials were near 0 mV, that is, 1.2 ± 1.0 mV, 2.0 ± 1.6 mV and −2.2 ± 1.8 mV, respectively. Error bars are indicated.

were purchased from Sigma Chemical (St. Louis, MO). Stock solutions of DIDS and SITS (10 mM) were prepared in 0.1 M $KHCO_3$ (pH = 8). $NiCl_2$ and $ZnCl_2$ (10 mM) were dissolved in normal saline.

Results

Electron microscopy. Under electron microscopic examination, the nearly homogeneous B95-8 cells had a round shape with a large nucleus/cytoplasm ratio. Large amounts of viral particles were found in the extracellular space. Some viral particles could be seen inside the intracellular vesicles and seemed to be readily excreted to the extracellular space (fig. 1). Some cells were lysed by viruses, and many viral particles were seen in the vicinity of the former intracellular area.

Channel conductance and channel abundance. Patch-clamp experiments revealed that small conductance channel activities were usually observed in a cell-attached configuration both in B95-8 and BJAB cells. Only in one patch was a large conductance channel activity corresponding to maxi-Cl channel in a B95-8 cell observed. Once the membrane patch was excised into the inside-out configuration, a large conductance channel activity with some subconductive openings was found, usually after application of depolarizing potential for a few seconds. To determine the single-channel conductance, currents were recorded in symmetrical 140 mM NaCl solutions. A representative recording from these solutions at different membrane potentials from a B95-8 cell is shown in figure 2A. The amplitude of the single-channel current was not changed by substituting the cytoplasmic Na^+ with K^+ ion. This was reflected in the I–V curves (fig. 2B) which were linear in these symmetrical Cl^- solutions, with a slope conductance of 316.7 ± 11.6 pS in NaCl (n = 16) and 297 ± 15.1 pS in KCl (n = 10) for B95-8 cells, and 343.6 ± 18.3 pS in NaCl (n = 3) for BJAB cells. The conductance and properties (voltage dependence, subconductive openings and anion selectivity) of the large channel activity were similar in both B95-8 and BJAB cells. Thus, we describe only the results obtained from B95-8 cells.

Up to 69% (42/61) of the inside-out patches in B95-8 cells expressed maxi-Cl channel activity. A continuous recording from an excised inside-out patch with 8 opening states is shown in figure 3A. At a transmembrane potential of +20 mV, outward-going currents corresponding to channel openings were observed. The total amplitude histogram constructed from 18 s of recording in figure 3A is shown in figure 3B. For BJAB cells, large conductance channel activity was present in 27% (3/11) of the inside-out patches.

Evidence for anion selectivity. The observed current reversal at 0 mV in symmetrical Cl^- solutions could indicate either an anionic or non-selective cationic channel. The results in figure 4 clearly show that the large conductance level was anion selective. Ion selectivity of

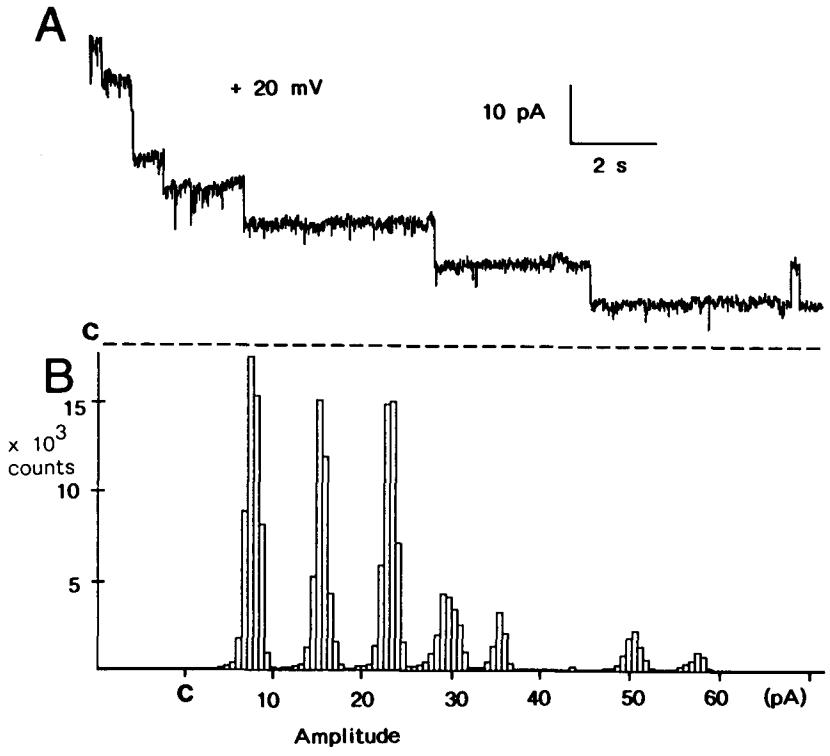

Figure 3. Eight similar channels observed in one membrane patch. (*A*) Continuous tracing of an inside-out patch with eight open levels. Outward-going currents were shown in symmetrical 140 mM NaCl solutions at +20 mV transmembrane potential. c and dashes indicate closed level. (*B*) Amplitude histogram constructed from the record in (*A*). The eight peaks show main open levels with a single-channel current about 8 pA.

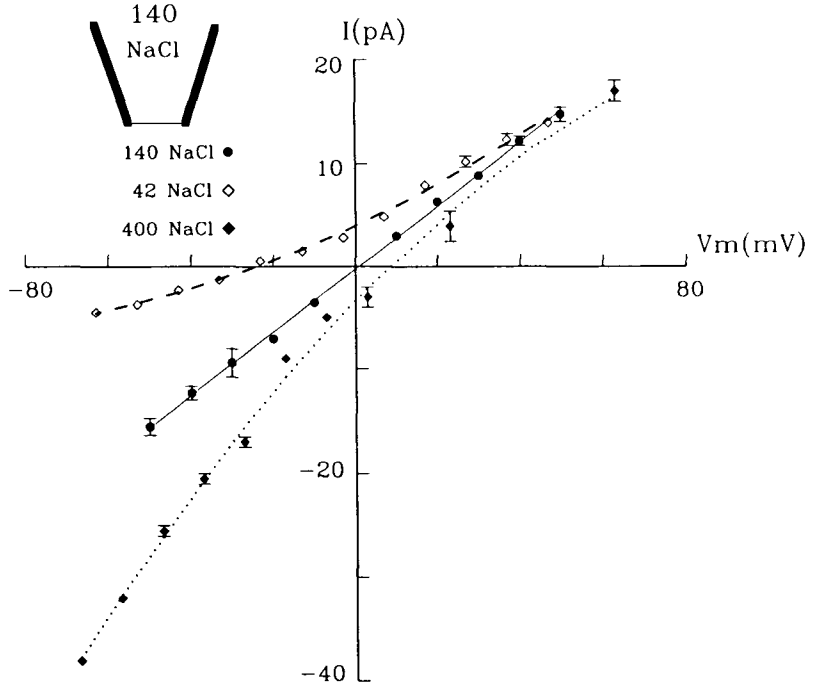

Figure 4. The large conductance channel is anion selective. Effect of ion concentration gradients on unitary I–V relationships obtained with excised, inside-out membrane patches. The cytoplasmic solutions contained 400, 140 and 42 mM NaCl. Isosmolality of the 42 mM NaCl saline was maintained by adding 200 mM sucrose. ● = 140 mM, ◇ = 42 mM, ◆ = 400 mM NaCl.

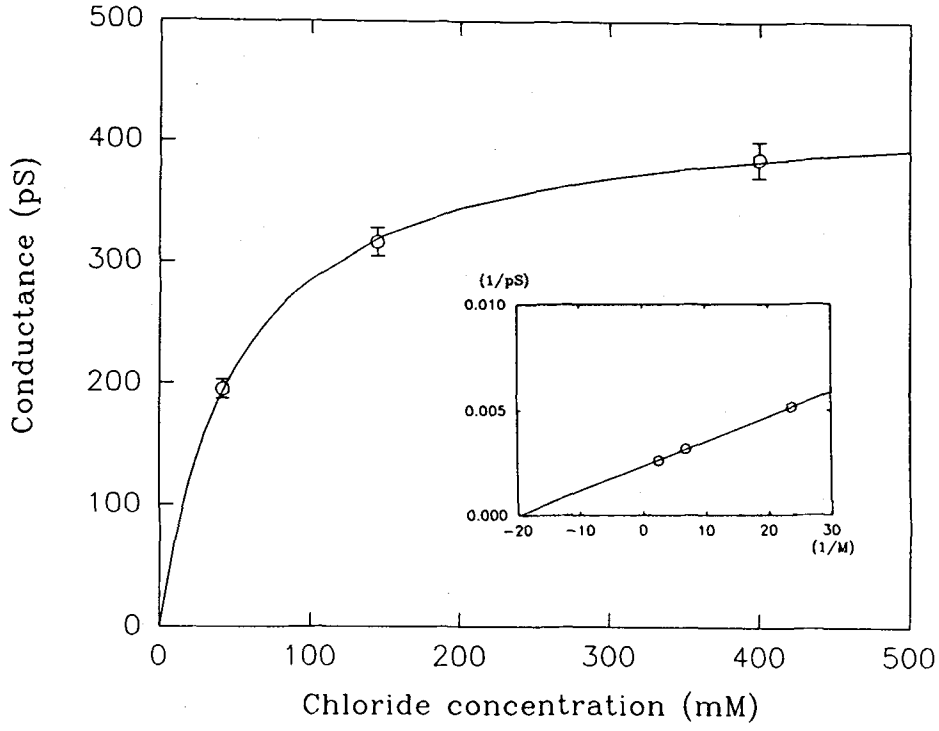

Figure 5. Conductance-versus-concentration relationship. The data were obtained on excised, inside-out patches with 140 mM NaCl in the pipette and different Cl concentrations in the cytoplasmic side. The data points in the Michaelis–Menten curve are mean ± SE. The curve is fitted by Michaelis–Menten equation. The inset shows a Lineweaver–Burk plot of the same data and the best fit of a linear regression. The units on these axes are M^{-1} and pS^{-1}.

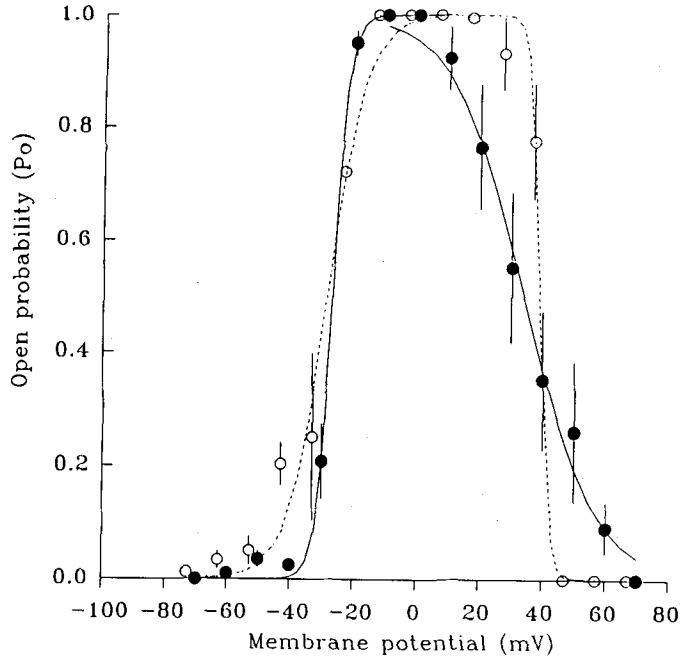

Figure 6. Voltage dependence of the opening probability of the maxi-Cl channel. Po was calculated from the proportion of time the channel spent in the open state of 20 s recording at a given voltage. Each point represents the mean ±SE. Solid lines represent experiments on excised, inside-out patches with 140 mM NaCl on both sides (n = 17). Dashed lines represent experiments with 42 mM NaCl on the cytoplasmic side (n = 6). The curves are fitted as the sum of two Boltzmann equations of the form:

$$P(V) = P_{max}/[1 + e^{(V - V_{1/2})/k_n}]$$

where $V_{1/2}$ is the voltage producing half-maximal probability and k_n is the slope factor corresponding to the voltage sensitivity of activation. The fitted values of $V_{1/2}$ and k_n were −26.9 mV and −2.4 mV, respectively, for the left side and +33.9 mV and +11.2 mV for the right side in symmetrical 140 mM NaCl. With cytoplasmic 42 mM NaCl, $V_{1/2}$ and k_n were −28.5 mV and −6.0 mV, respectively, for the left side and +38.9 mV and +1.6 mV for the right side.

Table 1. Reversal potential, conductance (γ_X) and relative permeability (P_X/P_{Cl}) of maxi-Cl channel for different anions.

Anion	Reversal potential (mV)	n	$\gamma_X(\gamma_X/\gamma_{Cl})$	P_X/P_{Cl}
I^-	6.2 ± 1.2	3	270.7 ± 12.0 (0.85)	1.3
Br^-	2.2 ± 0.4	3	325.0 ± 12.1 (1.03)	1.1
Cl^-	0	15	316.7 ± 11.6 (1.00)	1.0
F^-	-11.6 ± 2.2	3	209.8 ± 5.0 (0.66)	0.6
Gluconate	-34.1 ± 2.7	6	99.0 ± 10.5 (0.31)	0.2

this channel was tested by substituting the cytoplasmic solution with 42 mM and 400 mM NaCl. The unitary currents reversed at about -23.2 mV ($n = 5$) and $+12.4$ mV ($n = 3$), respectively. The shifts of the reversal potential approached the value predicted by the Nernst equation for an anion selective channel. The relative permeability of the channel for Cl^- over Na^+ was determined from experiments in which 42 mM NaCl cytoplasmic solutions were used. Using the Goldman–Hodgkin–Katz equation, a permeability ratio of $P_{Cl}:P_{Na} = 1:0.08$ was calculated after correction for activity coefficients.

The chord conductances for cytoplasmic 42 and 400 mM NaCl were 195.5 ± 8.0 pS and 385.7 ± 15.0 pS, respectively. The single-channel conductance was a function of the cytoplasmic Cl concentration. The conductance-versus-concentration relationship is shown in figure 5. We have fitted these data with a Michaelis–Menten equation in which the maximal conductance reached 434.2 pS and K_m was 52 mM. A Lineweaver–Burk plot is also shown in the inset.

Voltage-dependent gating. In the voltage range of about ± 30 mV, the maxi-Cl channel remained mostly in the open state (fig. 2A). Channel openings were hundreds of milliseconds long, separated only by brief closed intervals. They increased steeply with voltage, and the channel closed most of the time if the membrane potential was deflected beyond the ± 30 mV range. Figure 6 shows the probability of finding the channel in a conducting state when the membrane potential was switched between 0 mV and a different holding level. The opening probability was calculated as the proportion of time the channel spent in each 20 s of continuous recording. The P–V relationship was a bell-shaped curve with a maximum between -20 and $+20$ mV. The curve shifted when the cytoplasmic NaCl concentration changed from 140 mM (filled circles, solid lines) to 42 mM (open circles, dotted line). These relationships were well described as the sum of one rising and one falling Boltzmann distribution with slope factors of -2.4 mV and $+11.2$ mV for 140 mM NaCl, and -6.0 mV and $+1.6$ mV for 42 mM NaCl.

Selectivity and chloride channel blockers. The selectivity of the channel for Cl versus other anions was studied. Values of reversal potential were all relative to a rever-

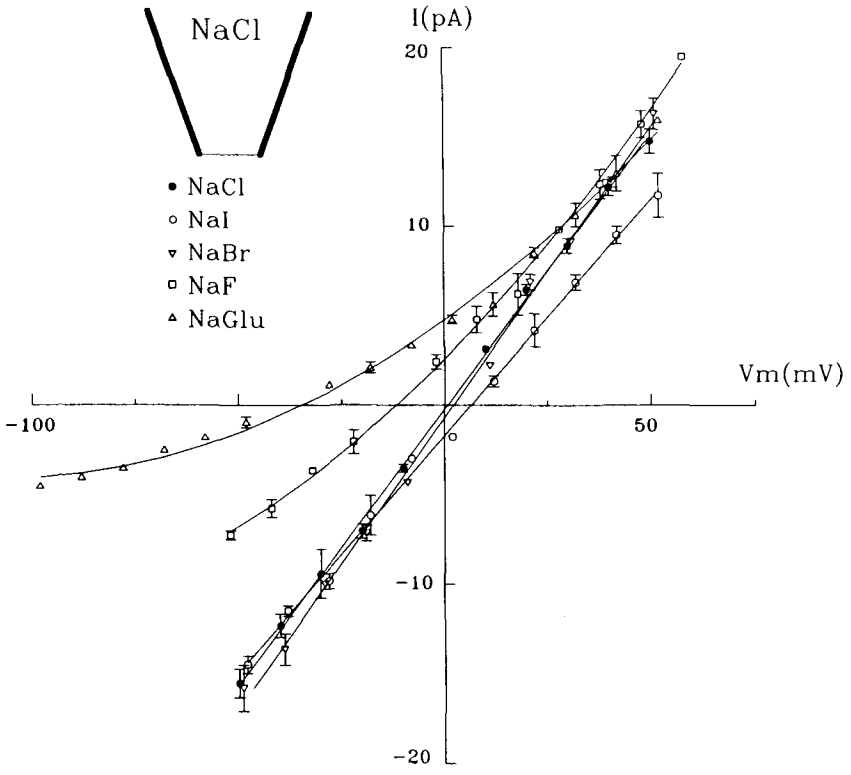

Figure 7. I–V relationships of different anions. The pipette contained 140 mM NaCl, and the cytoplasmic solutions contained equimolar amounts of anions. ● = NaCl, ○ = NaI, ▽ = NaBr, □ = NaF, △ = Na gluconate.

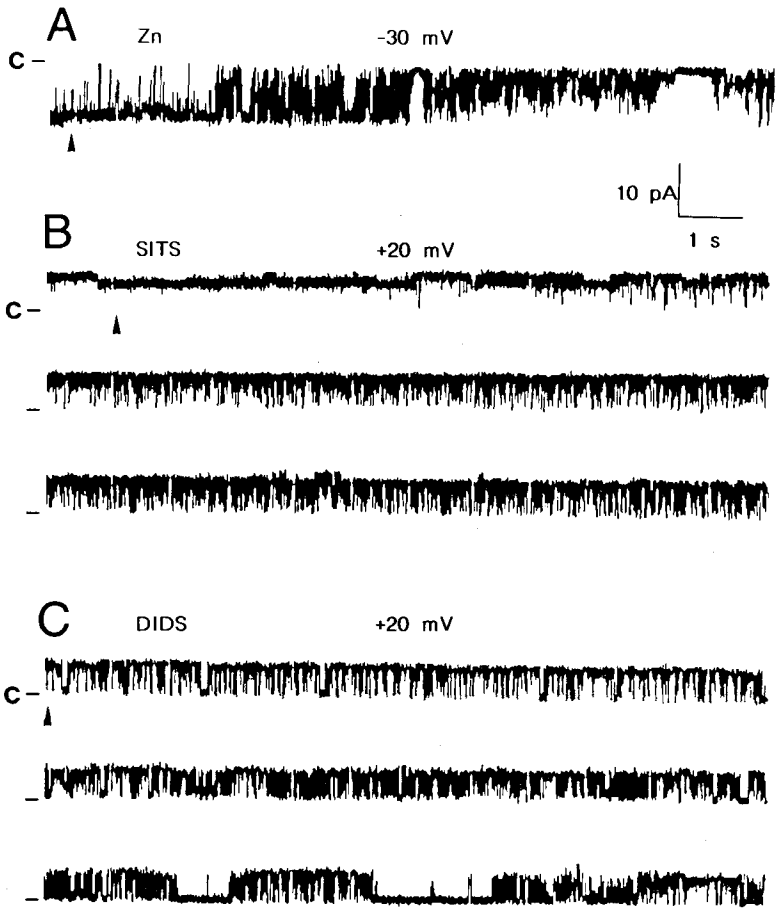

Figure 8. Block of the maxi-Cl channel by (*A*) 1 mM Zn^{2+}, (*B*) 100 µM SITS and (*C*) 100 µM DIDS in symmetrical 140 mM NaCl. The figure shows a time-dependent increase in channel flickering and closing. Arrowheads indicate adding blockers to cytoplasmic solution; c and dashes at the beginning of each trace indicate the closed level of the channel.

sal at 0 mV with 140 mM NaCl on both sides of the membrane. For the measurement of relative permeability, ion activities were calculated from activity coefficients after taking into account the degree of dissociation in tested solutions. Selectivities for different anions were determined by exposing excised patches to 140 mM NaCl on the extracellular side and tested anions on the cytoplasmic face. Each anion was substituted for Cl^- in equimolar amounts. The permeability ratio (P_X/P_{Cl}) was calculated from the Goldman–Hodgkin–Katz equation for monovalent anions. The details of the I–V relationship in different tested solutions are shown in figure 7. All results are summarized in table 1. The selectivity sequence based on permeability ratios was $I^- > Br^-, Cl^- > F^-$ > gluconate. Conductance ratios were calculated from the average single channel conductance, that is, the chord conductance calculated near the reversal potential. The conductance sequence was: $Br^-, Cl^- > I^- > F^-$ > gluconate (1.03: 1.00:0.85:0.66:0.31).

The bivalent metal ions were tested as potential blockers of the Cl channel as previously reported[16,17]. Zn^{2+} (fig. 8A) had a better blocking effect than did Ni^{2+} in 1 mM concentration. Inhibitors for Cl channel such as DIDS, SITS (fig. 8B, C) in 100 µM expressed flickering inhibition of the channel activity. All channel blockers were applied to the intracellular membrane face. All the blocking effects were reversible after washing.

Negative experiments. Changes in cytoplasmic Ca^{2+} concentration from 10^{-9} M to 10^{-3} M and pH from 6.2 to 8.2, and the application of 1 mM ATP, had no effect on channel behavior.

Discussion

Many cell lines established from EBV-transformed B lymphocytes have been used to study the life cycle and the pathogenesis of EBV. B95-8 is one of the most frequently used cell lines and serves as a high producer of EBV. Electron microscopic examination revealed that B95-8 cells produced large amounts of viral particles. Thus, the cell line was used as a representative of the EBV-infected cell to characterize the membrane channels and to compare with a non-EBV-infected B cell line – the BJAB cell.

Various types of ion channel in lymphocytes have been extensively investigated by the patch-clamp technique in recent years. Channels are thought to be involved in lymphocyte activation, proliferation, differentiation, cell volume regulation, cytotoxic function and mitogenesis[13,14]. So far, there has been no specific report on channels in EBV-infected cells. In the present study, we characterized the maxi-Cl channel on B95-8 cells.

Maxi-Cl channels are expressed ubiquitously in various cell types including lymphocytes[15–19], muscle cells[20,21] and various epithelial cells[22]. Three main features of the channel are: 1) its large unitary conductance, that is, 260–460 pS, and multiple levels of subconductance, 2) its narrow-ranged voltage dependence and 3) its activation after excision into inside-out patches at room temperature. The wide range of the conductance may be due to different experimental conditions. In our study, we have shown that the conductance is at least related to its cytoplasmic Cl concentration. Fitted to the Michaelis–Menten equation, the calculated maximal conductance reaches 430 pS (fig. 5). Multiple subconductive levels of the maxi-Cl channel may also influence the calculation of conductance. It has been reported that up to six co-channels may be present in this type of anionic channel[23]. Furthermore, single-channel conductance is temperature sensitive, increasing from about 125 pS at 5 °C to 250 pS at 20 °C and 350 pS at 37 °C in cell-attached patches of human T lymphocytes[17]. Certainly, the different conductances of maxi-Cl channels in various types of cells may indicate different types of the same class of anionic channel. The maxi-Cl channel of B95-8 cells showed similar voltage dependence of steady-state openings seen in inside-out patches from a murine hybridoma B cell line, human T lymphocytes and pulmonary alveolar epithelial cells. With excursions of ± 30 mV away from 0 mV, the channel closed in a time-dependent manner. The steady-state Po was a bell-shaped function centered on 0 mV and was well described as the sum of one rising and one falling Boltzmann function. The decrease in probability of finding the channel in the open state is best interpreted as one gate that closes at negative potentials and a second gate in series that closes at positive potentials[16]. The maxi-Cl channel is rarely active in the cell-attached configuration (only one patch in our experiment, and $<2\%$ in T lymphocytes) but stays in the long open state after excision at room temperature. This indicates that some intracellular controls of the channel opening must be functioning[16,17]. However, maxi-Cl channels could be observed in the cell-attached configuration at physiological temperatures (>32 °C) on previously quiescent patches in human T lymphocytes[18]. Thus, the maxi-Cl channel may not be as silent in vivo as we found in the cell-attached configuration at room temperature.

Until recently, no specific inhibitor of the maxi-Cl channel had been found. Bivalent metal cations such as Ni^{2+} or Zn^{2+}, and the universally used Cl channel blockers SITS and DIDS, may reversibly inhibit the activity of maxi-Cl channels[16,17]. The maxi-Cl channel found in B95-8 cells was inhibited by 1 mM Zn^{2+}, and 100 μM SITS or DIDS, but not obviously by 1 mM Ni^{2+}. The blocking effect was determined by detecting flickering current or long closing of the channel, which was not observed in the absence of inhibitors (fig. 8). Recent study of maxi-Cl channels in neuroblastoma cells has revealed that it is probably activated by thiamine triphosphate[24].

Although the maxi-Cl channel is found to be present in many types of cells, its physiological role is still being debated. It is thought to be involved in regulation of cell volume and may be particularly important in cells such as B lymphocytes which must exercise vigorous secretory activity. In view of its activation at more negative voltages, the maxi-Cl channel may also function in the control of the resting potential[16]. In general, the Cl current in lymphocytes is thought to be correlated with secretion and cell volume regulation, and with setting membrane potential[14]. Three other types of Cl channels in both human and murine B lymphocytes have been reported. CFTR has a conductance of 40–50 pS and is opened in excised patches by exposure to the catalytic subunit of cAMP-dependent protein kinase A plus ATP. This Cl channel is defective in epithelial cells of cystic fibrosis patients[9]. Using whole cell and perforated patch recording techniques, volume-sensitive Cl channels in T and B lymphocytes are characterized as having an unitary chord conductance of only 2 pS at -80 mV in the presence of symmetrical 160 mM Cl^{-}[25]. Another 128 pS anion channel is also less frequently observed in resting murine B lymphocytes[19].

In the absence of a monoclonal antibody to the channel protein, or high-affinity ligands, the relative abundance of maxi-Cl channels on various types of cells can only be estimated from the probability of their presence in patches. Hals et al. calculated a channel density of 1 channel per 6.97 μm^2 in sarcoplasmic reticulum[26], and Gray et al. 1 channel per 10–100 μm^2 in Schwann cells[27]. In B95-8 cells, maxi-Cl channels were present in at least 69% (42/61) of excised inside-out patches, and up to eight channels could be found in one patch (~ 1 μm^2) (fig. 3). In comparison with BJAB cells or previously reported intact human T lymphocytes and resting murine B lymphocytes, similar currents were found in only 27% (3/11) or 37% (114/308) and 38% (87/221) of excised patches under the same experimental conditions. Evidently, more maxi-Cl channels were present in the membranes of B95-8 cells.

Different channel densities across cell lines may be due to the different origins of cell lines, different degree of infolding of each cell type's plasma membrane or even

the length of time in culture. Thus, it may be premature to conclude that the phenomena described here are related to EBV immortalization or virus replication. Yet, the consistent probability of detecting maxi-Cl channels by the patch-clamp technique on different non-EBV-infected lymphocytes led us to speculate that the relative abundance of the channels on B95-8 cells may correlate with EBV infection and/or virus excreting ability.

In summary, we described a careful analysis of maxi-Cl channels in the cell line B95-8 transformed by EBV. We demonstrated the anion selectivity, the voltage dependence of channel gating and relative abundance of the channel in these cells. Further experiments, for example, to detect increased density of channels on B lymphocytes after EBV infection, will be needed to solidify the connection between EBV infection and the maxi-Cl channel.

Acknowledgements. We are grateful to Professor J. Y. Chen of the microbiological department for supplying the B95-8 and BJAB cell lines, Mr Y. C. Chen for technical assistance in preparing the electromicroscopic photographs, and Professor P. Tran Ba Huy of Lariboisière Hospital, Paris, for helpful comments on the manuscript. This project was supported by a grant from the National Science Council of Taiwan (NSC-83-0412-B002-023) to T. H. Yeh.

1 Old, L. J., Boyse, E. A., Oettgen, H. F., de Harven, E., Geering, G., Williamson, B., and Clifford, P., Proc. natl Acad. Sci. USA *56* (1966) 1699.
2 Tu, S. M., in: Proceedings of Eighth International Congress of Oto-Rhino-Laryngology, vol. 113, p. 184. Excerpta Medica Foundation, Amsterdam, International Congress Series 1965.
3 Miller, G., and Lipman, M., Proc. natl Acad. Sci. USA *70* (1973) 190.
4 Miller, G., Shope, T., Coope, D., Waters, L., Pagano, J., Bornkamm, G. W., and Henle, W., J. expl Med. *145* (1977) 948.
5 Birkenbach, M., Josefson, K., Yalamanchili, R., Lenoir, G., and Kieff, E., J. Virol. *67* (1993) 2209.
6 Wang, D., Liebowitz, D., and Kieff, E., Cell *43* (1985) 831.
7 Sugdan, B., Cell *57* (1989) 5.
8 Bernt, L. H., Butler, J. L., Woods Jr., W. T., and Bubien, J. K., J. Immun. *145* (1990) 2381.
9 Chen, J. H., Schulman, H., and Gardner, P., Science *243* (1989) 57.
10 Wang, C., Takeuchi, K., Pinto, L. H., and Lamb, R. A., J. Virol. *67* (1993) 5585.
11 Pinto, L. H., Holsinger, L. J., and Lamb, R. A., Cell *69* (1992) 517.
12 Hamill, O. P., Marty, A., Neher, E., Sakmann, B., and Sigworth, F. S., Pflügers Arch. *391* (1981) 85.
13 Premack, B. A., and Gardner, P., J. clin. Immun. *11* (1991) 225.
14 Gallin, E. K., Physiol. Rev. *71* (1991) 775.
15 Hwang, T. C., Lu, L., Zeitlin, P. L., Gruenert, D. C., Huganir, R., and Guggino, W. B., Science *244* (1989) 1351.
16 Bosma, M. M., J. Physiol., Lond. *410* (1989) 67.
17 Schlichter, L. C., Grygorczyk, R., Pahapill, P. A., and Grygorczyk, C., Pflügers Arch. *416* (1990) 413.
18 Pahapill, P. A., and Schlichter, L. C., J. Memb. Biol. *125* (1992) 171.
19 McCann, F. V., McCarthy, D. C., and Noelle, R. J., J. Memb. Biol. *114* (1990) 175.
20 Woll, K. H., Leibowitz, M. D., Neumcke, B., and Hille, B., Pflügers Arch. *410* (1987) 632.
21 Soejima, M., and Kokubun, S., Pflügers Arch. *411* (1988) 304.
22 Hayslett, J. P., Gögelein, H., Kunzelmann, K., and Greger, R., Pflügers Arch. *410* (1987) 487.
23 Krouse, M. E., Schneider, G. T., and Gage, P. W., Nature, Lond. *319* (1986) 58.
24 Bettendorff, L., Kolb, H.-A., and Schoffeniels, E., J. Memb. Biol. *136* (1993) 281.
25 Lewis, R. S., Ross, P. E., and Cahalan, M. D., J. gen. Physiol. *101* (1993) 801.
26 Hals, G. D., Stein, P. G., and Palade, P T., J. gen. Physiol. *93* (1989) 385.
27 Gray, P. T. A., Bevan, S., and Ritchie, J. M., Proc. R. Soc. Ser. B *221* (1984) 395.